Scientific Research Publishing

Open Journal of Geology, 2023, 13, 1177-1194
https://www.scirp.org/journal/ojg
ISSN Online: 2161-7589
ISSN Print: 2161-7570

Aeromagnetic Imagery as a Tool to Help Identify the Structures Controlling the Emplacement of the Kenieba Kimberlite Pipes (Western Mali, West African Craton)

Baco Traore[1,2], Gbele Ouattara[1*], Marc Ephrem Allialy[3], Ousmane Wane[4], Mohamed Moustapha Ndam Njikam[5], Adama Youssouf Kone[6], Souleymane Sangare[2]

[1]Civil Engineering, Geosciences and Geographic Sciences Laboratory, Yamoussoukro, Côte d'Ivoire
[2]Bamako, Mali
[3]UFR-STRM, University of Cocody, Abidjan, Côte d'Ivoire
[4]Laboratory of Mineralogy and Petrology, Faculty of Sciences and Techniques, University of Sciences, Techniques and Technologies of Bamako, Bamako, Mali
[5]School of Geology and Mining Engineering, University of Ngaoundere, Ngaoundere, Cameroon
[6]Faculty of Sciences and Technics (FST), University of Sciences, Technics and Technologies of Bamako (USTTB), Bamako, Mali
Email: *gbele.ouattara@yahoo.fr

How to cite this paper: Traore, B., Ouattara, G., Allialy, M.E., Wane, O., Njikam, M.M.N., Kone, A.Y. and Sangare, S. (2023) Aeromagnetic Imagery as a Tool to Help Identify the Structures Controlling the Emplacement of the Kenieba Kimberlite Pipes (Western Mali, West African Craton). *Open Journal of Geology*, **13**, 1177-1194.
https://doi.org/10.4236/ojg.2023.1311050

Received: September 28, 2023
Accepted: November 19, 2023
Published: November 22, 2023

Abstract

A kimberlite field, represented by fertile and sterile kimberlite pipes (chimneys) is located in the region of Kenieba (West Mali, Kédougou-Kenieba inlier, West African Craton). Thirty pipes and kimberlite dykes have been identified in the birimian formations, composed mainly of metasediments and granitoids, covered by sedimentary formations (sandstones and conglomerates) of Neoproterozoic age. All these formations are injected with dykes and doleritic sills of Jurassic age. The study of kimberlite pipes is still stammering in Mali, and thus no previous study has allowed to characterize the structures controlling their implementation. The reinterpretation of aeromagnetic data validated by field work indicates that the major structures of the Kenieba region are oriented NNE-SSW, NE-SW, E-W and NW-SE. These structures (faults and kimberlite pipes) are often associated with dolerite dykes, which would imply an injection of dolerite magma into the other formations. The location of the known kimberlite pipes makes it possible to say that the direction NW-SE is the most favorable for the exploration of kimberlites in the region of Kenieba.

Keywords

Kimberlite Pipes, Doleritic Dykes, Fractures, Aeromagnetism, Kenieba, Mali

1. Introduction

The Kenieba kimberlite field in western Mali (West African Craton, WAC) is characterized by kimberlite pipes (chimneys), gem-quality diamonds and indicator minerals [1]. The results of previous works show that some of the highlighted pipes contain microdiamonds with low economic potential, and that miners frequently announce the discovery of large diamonds in the alluvium.

Intrusions located, approximately, more than ten kilometers from the city of Kenieba, were highlighted by BRGM during the year 1958. These rocks have been identified as kimberlites. This discovery caused a sudden and growing interest in this area, for exploration in the 1960s. The age of implementation of kimberlite intrusions in West Africa was determined by the work of [2], who used the Rb/Sr method on phlogopite. They got an age of 1072 Ma for a chimney in Sékonomata near Kenieba. This age corresponds to the establishment of the Neoproterozoic sandstone formations crossed by the intrusions of doleritic sills and dykes [3].

Structurally, the work of [4] shows, through a geophysical study, that the major structures affecting this part of the West African craton are linked to: 1) the opening of the Atlantic Ocean with a NW-SE orientation; 2) Pan Africa with N-S to NNE-SSW guidelines; 3) some structures associated with the establishment of the Taoudéni basin during a rifting with NE-SW and E-W orientations; 4) Eburnean orogenesis with NW-SE orientations at ENE-WSW. The works on swarms of mafic dykes indicate NE-SW to NW-SE directions [5]. The use of aeromagnetic data revealed several directional structures NW-SE [6], N-S (Senegalese-Malian shear zone in the western part of the study area and NE-SW (Kédougou-Kenieba shear zone) [7].

The objective of this work is to understand the conditions of formation of Kenieba kimberlites in order to bring new arguments for the diamond exploration sector in Mali. Aeromagnetic images were therefore used to understand the structures favoring the formation of these kimberlites. Known pipes are interpreted and new targets are proposed.

2. Geological and Tectonic Settings

The study area belongs geologically to the Kédougou-Kenieba Inlier (KKI), which is included in the WAC, of which it formed a central-western margin [8] [9]. The KKI is made up of metavolcanic, metavolcano-sedimentary and intrusive formations [10] [11], as shown in **Figure 1**.

The Birimian formations are deformed and metamorphosed, mainly in greenschist facies, and were structured during the Eburnean orogeny, which is dated at around 2270 - 1960 Ma [9]. They are bounded to the east by the vast sedimentary cover of the Neoproterozoic domain. The kimberlite pipes intersect the Paleoproterozoic formations of the Kenieba plain and the Neoproterozoic formations of the Tambaoura [12].

Kimberlites from Mali are intrusive in both Birimian rocks and Neoproterozoic sandstones, but have greater abundance in the Birimian domain.

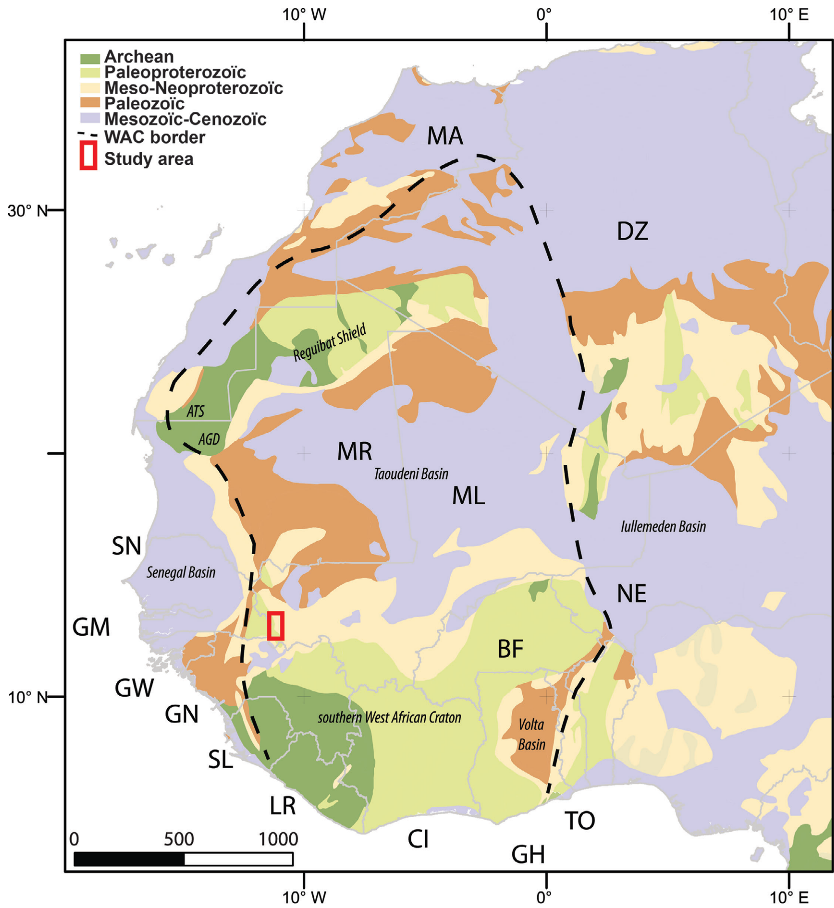

Figure 1. Map of West Africa showing the ages of the major terranes, modified from the Geological Survey of Canada 1:35 M map of the world [14], in [3], showing the approximate limit of the present day WAC as a heavy dashed line (after [15]). The study zone is indicated in red rectangle. AGD: Ahmeyim Great Dyke; ATS: Aousserde Tichla swarm. *Two-letter country codes*: *BF*: *Burkina Faso*; *CI*: *Cote d'Ivoire*; *DZ*: *Algeria*; *GH*: *Ghana*; *GM*: *The Gambia*; *GN*: *Guinea*; *GW*: *Guinea Bissau*; *LR*: *Liberia*; *MA*: *Morocco*; *ML*: *Mali*; *MR*: *Mauritania*; *NE*: *Niger*; *SL*: *Sierra Leone*; *SN*: *Senegal*; *and TO*: *Togo*.

The first discovery of diamonds in the Kenieba region was made by gold miners in 1954. Subsequently, several kimberlite pipes were identified as part of the extensive exploration work [12]. The diamond of the Kenieba region is found in alluvium and/or kimberlite pipes.

Knowledge of Mali's geology has been considerably enhanced by a cooperative program between the government of the Republic of Mali and the BRGM/Geosystem Maps consortium, which led to the production of the 1:200,000 geological map [13]. The rocks of the Malian part of the Kédougou-Kenieba inlier are associated with the Eburnean orogeny dated approximately between 2000 and 2600 Ma.

Haggerty [16] estimated that the kimberlites of Mali were "associated" with those of Liberia and that all were structurally controlled by the Archean subsoil complex of the Leo Ridge. This author clearly identifies a structural relationship between the Liberian kimberlites and that of Kenieba. Although the majority of known kimberlites in West Africa are restricted to the Liberian domain, diamonds have however been discovered in Birimian suggesting that an overall distribution of kimberlites in this part could be expanded beyond the Liberian (**Figure 2**) [17] [18] [19] [20] [21].

A large portion of the West African kimberlites is dyke type that is associated with structures with an overall E-W trend. But conjugate trends have been mapped in Guinea with approximately N-S or NE-SW directions [22]. In Mali, we have NW-SE and E-W (Delys Dyke) management. Major structures (shear zones, faults, fractures, sills and doleritic dykes) have N-S, NE-SW, NW-SE and E-W directions [4] [5] [6] [7] (**Figure 3**).

3. Data Used and Methodology

3.1. Data

The magnetic data used in this study come from aeromagnetic surveys carried out between 1996 and 1997 by the company High-Sense Geophysics, on behalf of the Ministry of Mines, Energy and Water of the Republic of Mali. The aeromagnetic coverage was conducted at a flight altitude of 100 m following the N65E oriented profiles and spaced 200 m apart, with a magnetometer recording sensitivity of more or less 0.001 nT.

After correction of the measurements due to the temporal variation of the magnetic field, the data of total magnetic intensity (TMI), were deducted by making the difference between the measured field and the fraction of the regional field taken from the 1995 IGRF model. The TMI grid was then developed using the minimum curvature as the interpolation method for a 100 m sampling step (**Figure 4(a)**). A reduction at the pole was applied to the TMI grid in order to bring back the anomalies observed vertically from their causative sources. This was done by selecting a point in the center of the magnetic anomalies map (−11.25˚E and 12.92˚N), with tilt values (I = 4.509˚) and declination (D = −8.093˚) from the 1995 IGRF model. The RTP map obtained, which is the basic data used for the different treatments performed in this study, is given in **Figure 4(b)**.

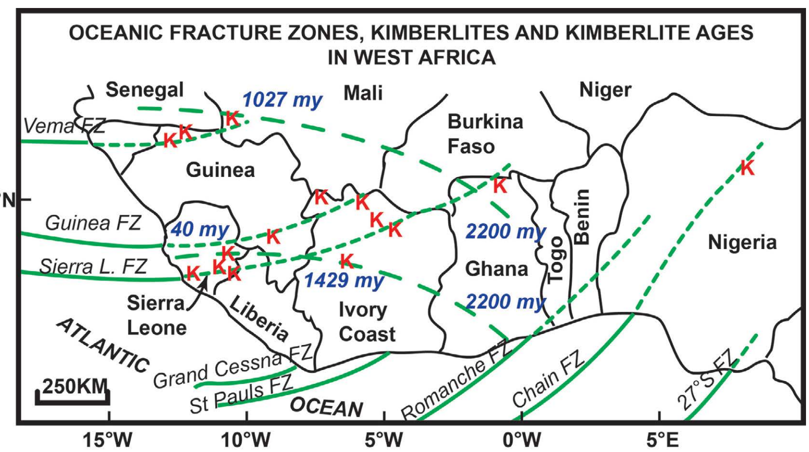

Figure 2. Regional repartition of assumed kimberlites (K) in West Africa [17].

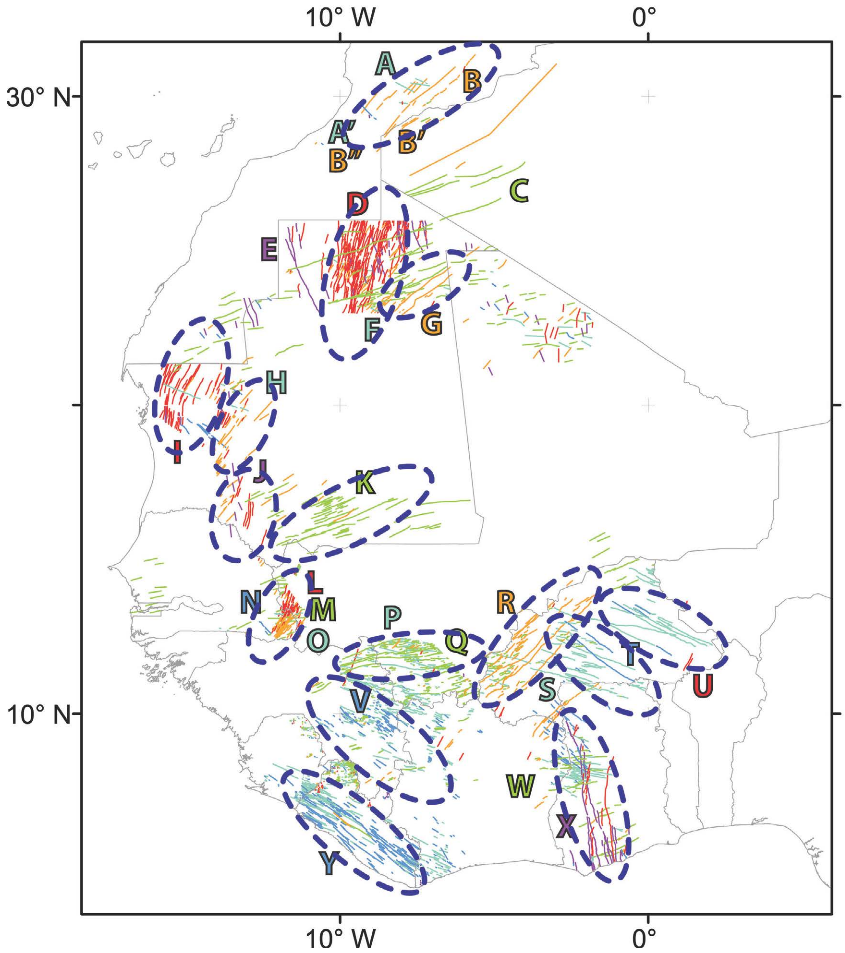

Figure 3. Global repartition and orientation of West African mafic dykes as mapped in this and previous studies [3], modified.

3.2. Methodology

3.2.1. Spectral Analysis

Spectral analysis has been widely used by many authors to determine the depth of magnetic and gravimetric anomalies [23]-[32].

Magnetic anomalies can be properly treated as a spatial series applicable to Fourier synthesis and analysis without affecting the intrinsic appearance of the anomalies [26] [27]. Spectral analysis does not require a priori knowledge of the geometry or density contrast of the bodies responsible for the observed anomalies. It simply requires the study of spectral energy as a function of wavelength [29] [30] [32] [33]. Near-surface sources will thus give a flatter power spectrum, while deeper sources will give a steeper power spectrum [26] [27]. The depth (h) of an interface can be obtained using the formula of [23] given by "Equation (1)".

$$h = \Delta(\mathrm{Log}E)/4\pi\Delta(n) \tag{1}$$

where E represents the energy spectrum; $\Delta(\mathrm{Log}E)$ is the variation of the logarithm of the energy spectrum in the frequency interval $\Delta(n)$.

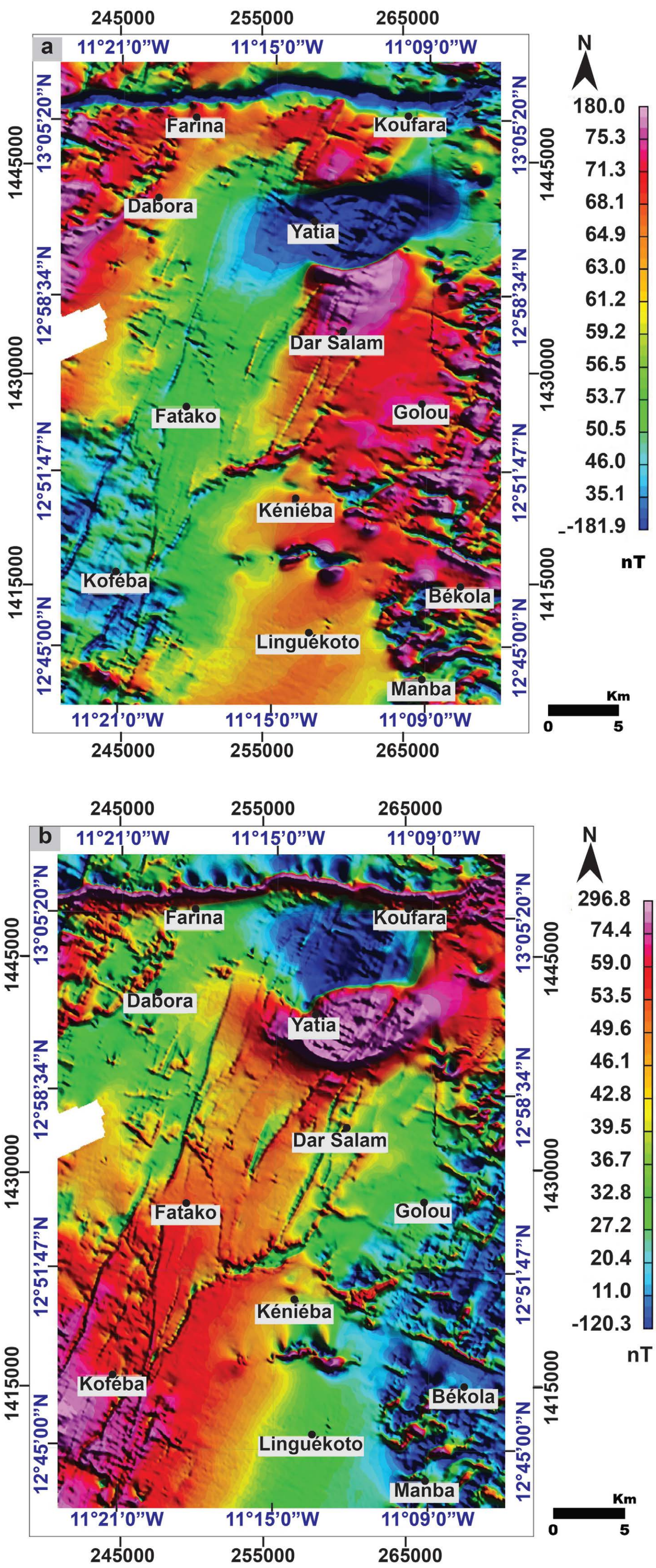

Figure 4. (a) Total Magnetic Intensity (TMI) map; (b) Map of the Reduced to The Pole (RTP).

3.2.2. Vertical Derivative (DZ) and Analytical Signal (SA)

The vertical derivative filter amplifies the effect of surface sources by mitigating the effect of deep sources. This filter enhances the relief of a near-surface anomaly by allowing its geometric boundaries to be further defined [34] [35]. In this study, it is mainly used in structural interpretation and the relationship between deep and superficial structures. The operator of the vertical derivative of order n is given by Equation (2).

$$O_{DV} = \sqrt{\left(k_x^2 + k_y^2\right)^n} \tag{2}$$

Regarding the analytical signal method, it was first described by [36] [37] [38] as a complex field deriving from a complex potential. This method does not require knowledge of source parameters or ambient magnetic field parameters [32]. It is very effective in highlighting areas of intrusion or geological contacts. This technique has been used in many studies, not only for structural interpretation but also to highlight areas of deep geological formations or contacts or under cover [32] [39].

The mathematical expression of the amplitude of the analytical signal (AAS) proposed in 1984 by Nabighian [38] and which is a function of the horizontal derivative (following x and following y) and the vertical derivative z is given by Equation (3).

$$\left\|\mathrm{AAS}(x,y)\right\| = \sqrt{\left(\frac{\partial f(x,y)}{\partial x}\right)^2 + \left(\frac{\partial f(x,y)}{\partial y}\right)^2 + \left(\frac{\partial f(x,y)}{\partial z}\right)^2} \tag{3}$$

3.2.3. Euler Deconvolution (ED)

This technique is very often used to automatically estimate the location and depth of magnetic and gravimetric sources [30] [39] [40] [41] [42]. This method was established by [43] and was applied mainly to real magnetic data along the profiles.

Using Thompson's approach [43] [44] developed the equivalent grid method. The mathematical expression of Euler 3-D deconvolution given by [44] is represented by Equation (4).

$$\frac{(x-x_0)\partial T}{\partial x} + \frac{(y-y_0)\partial T}{\partial y} + \frac{(z-z_0)\partial T}{\partial z} = N(B-T) \tag{4}$$

With: (x_0, y_0, z_0): position of the anomaly source; (x, y, z): position of the observer; T: magnetic or gravimetric field detected at (x, y, z); B: regional value of the total field; N: degree of homogeneity often called structural index.

4. Results

On the RTP map (**Figure 4(b)**), important positive and negative anomalies of very varied shapes and intensities can be observed:

- The negative anomalies whose amplitudes vary from −120.3 to 0 nT are located mainly in the north of Yatia and in the SE frame of the study area. These are diamagnetic formations that can correspond to sedimentary formations. Although, uniform in their distribution, these areas of negative anomalies are littered with positive anomalies of very small extent that may correspond to volcanic formations or intrusive bodies;

- Positive anomalies with amplitudes ranging from 39.5 to 296.8 are much more widespread and correspond to ferromagnesian materials. They have both circular (Yatia anomaly) and rectilinear (E-W anomaly of the Farina-Koufara axis north of the study area). Circular anomalies may correspond to granitic intrusion zones like the positive Yatia anomaly, while rectilinear anomalies may be interpreted as lineaments, fault zones or doleritic dykes. On the NE-SW anomaly corridor passing through the Kofeba-Fatako axis, a set of structural features can be observed from the relief of rectilinear anomalies and these geological structures can be interpreted using specific filters.

In order to evaluate the average maximum depth associated with the RTP grid (**Figure 4(b)**) and thus define the different depth domains, a 2D radial spectrum was applied to the RTP grid. The spectrum obtained (**Figure 5**) highlights the average depth slices (roof and wall) corresponding to the four information domains searched. According to this spectrum, the average maximum depth of the deep sources is 1339.65 m, while those of the intermediate sources are, in descending order, 206.61, 95.62 m and 17.36 m (**Figure 5**). Unlike the others, the 17.36 m depth corresponds to that of near-surface formations and structures, and is the least accurate because it incorporates noise (or Nyquist frequency) generated by the method used as one approaches the surface.

To enhance the relief of magnetic anomalies associated with geological structures, a vertical derivative (DZ) filter was applied to the RTP grid. Analysis of the resulting DZ map (**Figure 6(a)**) reveals a series of structural features. Despite a decrease in intensity and volume, the circular positive anomaly associated with the Yatia granite is visible on the DZ map, demonstrating that this granitic formation

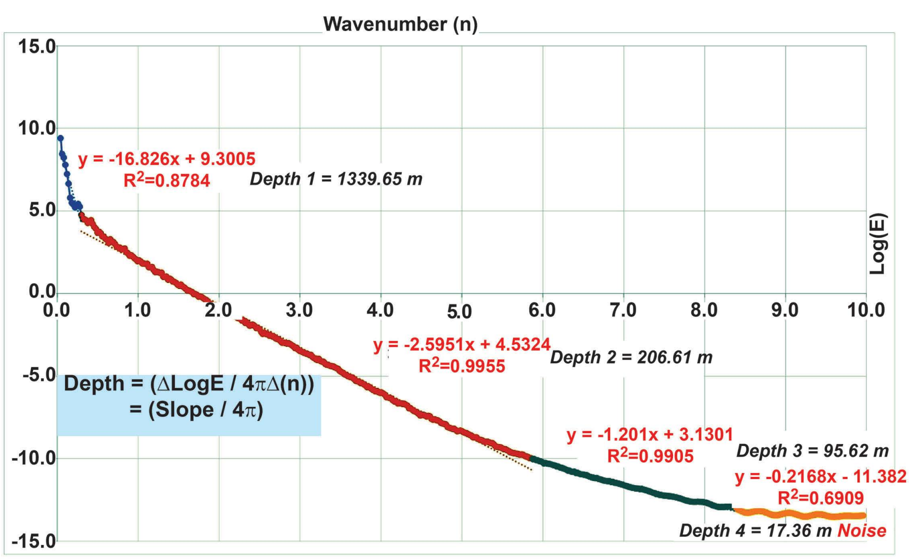

Figure 5. Result of spectral analysis of the RTP grid.

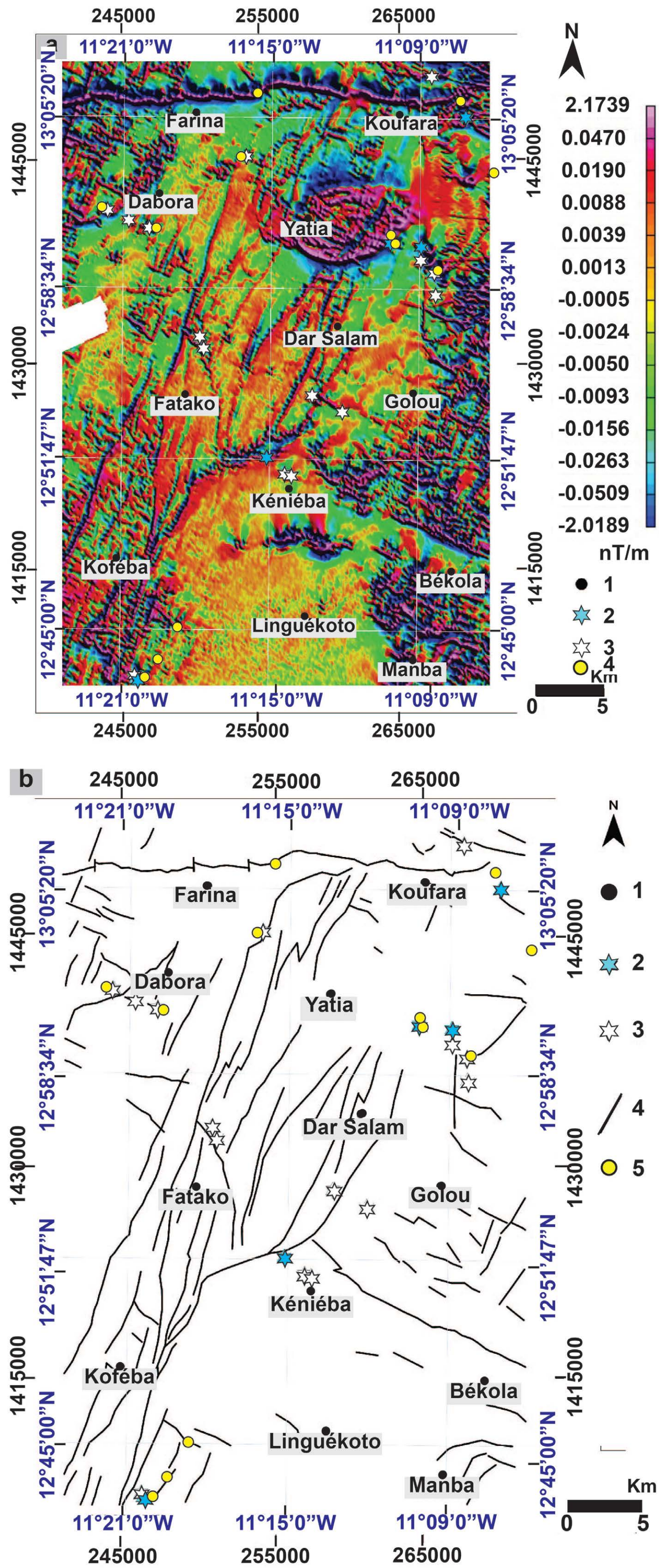

Figure 6. (a) Vertical derivative map; (b) Synthesis structural map. 1: *Names of localities*; 2: *Samples of diamondiferous kimberlites*; 3: *Samples of non-diamondiferous kimberlites*; 4*a and* 5*b*: *Dolerites*; 4*b*: *Interpreted faults*.

outcrops at the surface. The positive E-W anomaly along the Farina-Koufara axis has also decreased in intensity and volume. The structural feature enabling us to identify the line of this E-W anomaly on the DZ map, leads us to understand that it is covered by superficial deposits but that its roof is fairly close to the surface.

The general interpretation of the various structural features of the DZ map has led to the development of a synthetic structural model (**Figure 6(b)**). This model, whose major axis in the shape of a ponytail is oriented NE-SW, defines a set of dexter and sinistral wrench faults.

Correlative analysis of the spatial distribution of diamondiferous and non-diamondiferous kimberlite samples collected in the study area, with the interpreted structures (**Figure 6(a)** and **Figure 6(b)**), shows that they are predominantly located in fault zones. As kimberlites are generally associated with deep-seated structures, to identify faults in the structural model in **Figure 6(b)** that meet this criterion and thus delineate the geometry of target anomalies, an analytical signal (AS) filter was applied to the RTP grid (**Figure 7(a)**).

Analysis of the AS map shows that most of the structures interpreted on the DZ map correspond at depth to anomalous zones that may be associated with the dolerite dykes observed in the study area. The distribution of diamondiferous and non-diamondiferous kimberlite samples on the AS map shows that these samples are also related to the doleritic dyke anomalies highlighted. These dykes, which are potential diamondiferous targets in the study area, are thought to be the product of a mixture of doleritic and diamondiferous magma lodged in fault zones.

A categorization of the AS grid into ranges of 0.04 nT/m combined with the spatial distribution of the kimberlite samples enabled us to define the geometry of the various diamondiferous targets (**Figure 7(b)**) and their relationship with the structural model in **Figure 6(b)**. To assess the depth of interpreted faults and dykes, the Euler deconvolution method was applied to the RTP grid for specific Euler parameters (structural index N = 0.1; tolerance Z = 5% and window W = 8).

The distribution of Euler solutions compared with the plots of the various structures (**Figure 8(a)** and **Figure 8(b)**), shows that the depth of the interpreted structures varies from surface to a maximum depth of 400 m. A complete categorization of the AS grid into ranges of 0.005 nT/m, based on the variation in magnetic relief, shows the relationship between the interpreted structures and the basic geological formations of the study area (**Figure 9(a)** and **Figure 9(b)**).

5. Discussion

The Kenieba region (straddling the Birimian domain and the Neoproterozoic cover) was the site of diamond mining in the 1960s. However, very little exploration works on the primary origin of the diamond has been completed. Earlier work on the kimberlites of the West African craton showed varied ages [17], as well as varied ages of the mafic dykes more or less associated with certain kimberlites [3]. The reinterpreted aeromagnetic data bring new insights, both structurally, and in terms of prospecting targets for kimberlites.

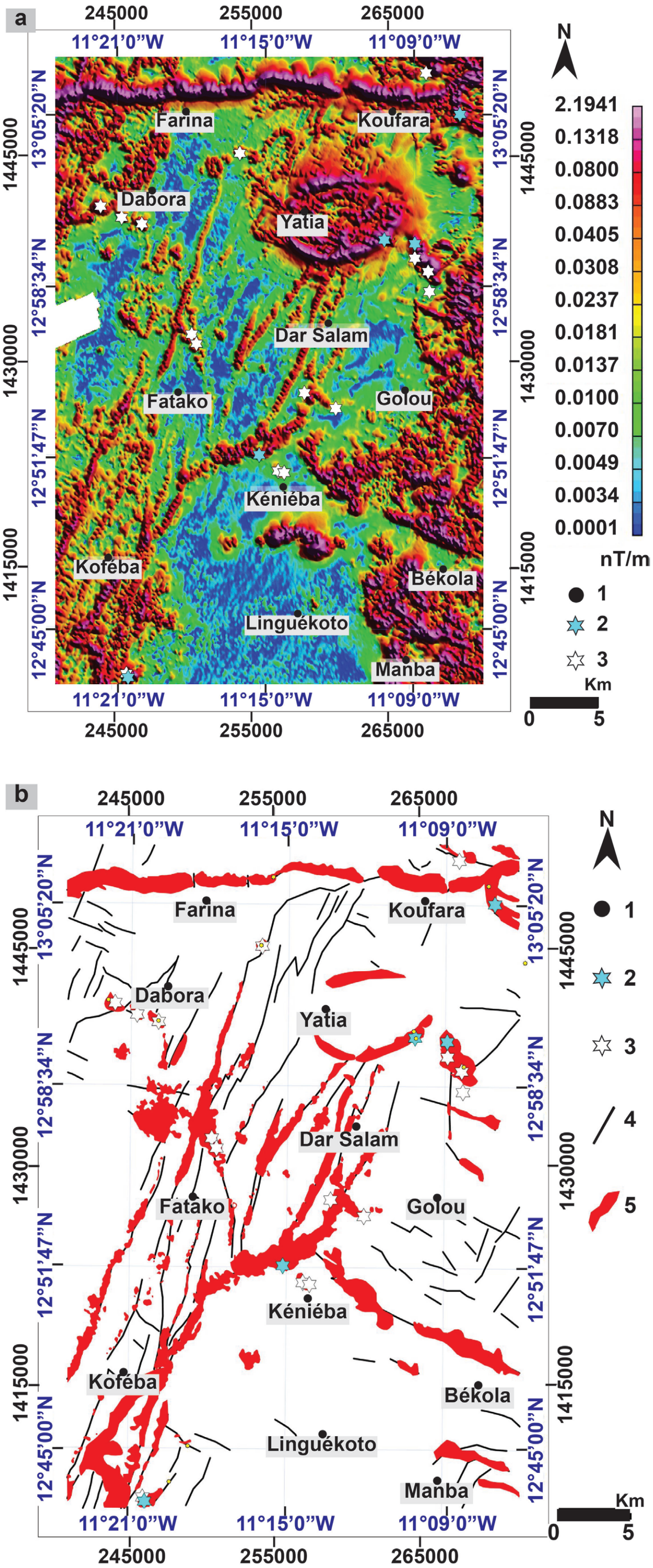

Figure 7. (a) Analytical signal map; (b) Structural map and diamondiferous targets. 1: *Locality names*; 2: *Kimberlite pipes*; 3: *Non-diamond-bearing kimberlite samples*; 4: *Interpreted faults*; 5: *Dykes derived from a mixture of doleritic and diamond-bearing magma*.

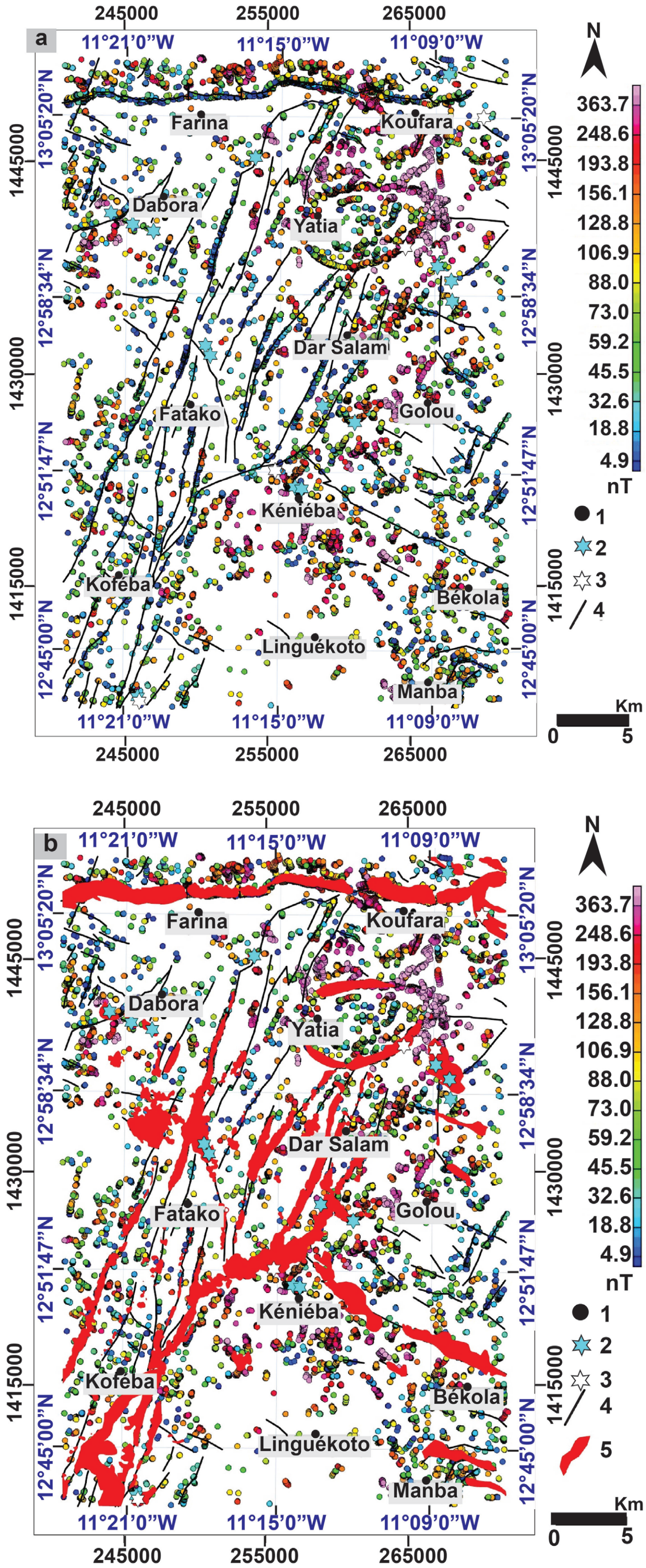

Figure 8. (a) Analytical signal map; (b) Structural map and diamondiferous targets. 1: *Locality names*; 2: *Kimberlite pipes*; 3: *Non-diamond-bearing kimberlite samples*; 4: *Interpreted faults*; 5: *Dykes derived from a mixture of doleritic and diamond-bearing magma*.

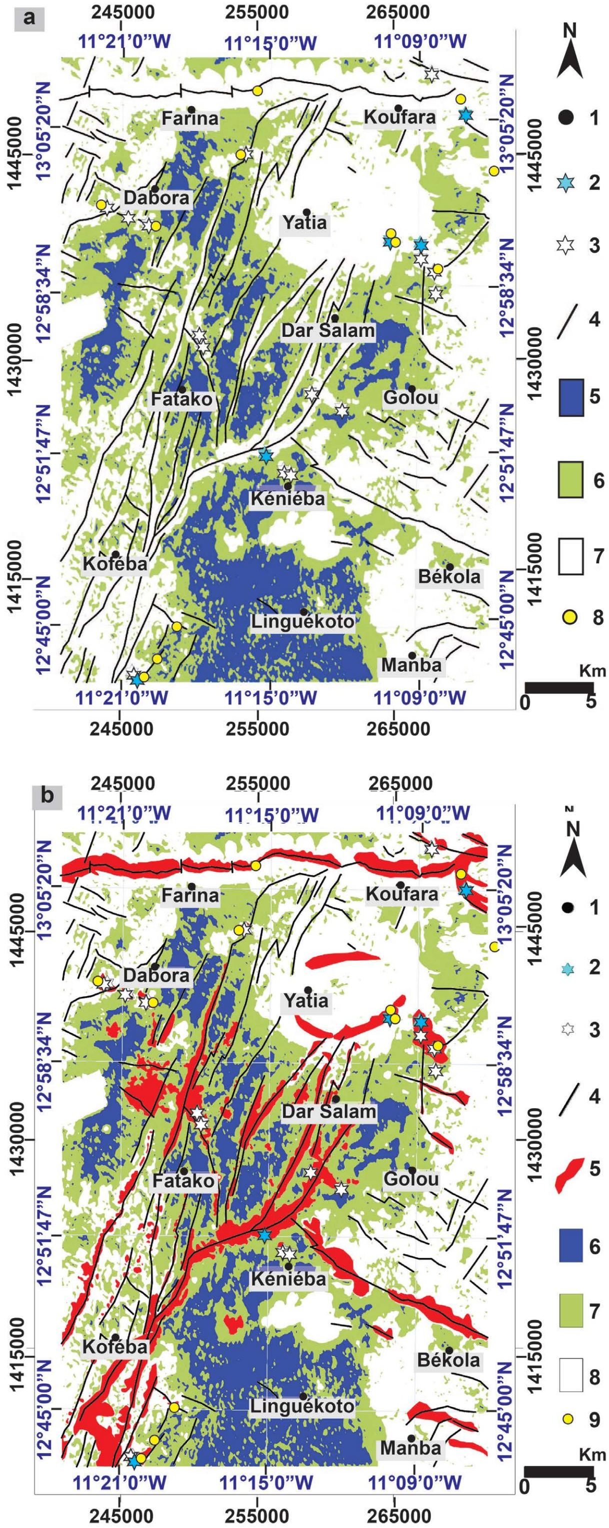

Figure 9. (a) Base formations associated with the synthesis structural model; (b) Base formations associated with the structural model and diamondiferous targets. 1: *Locality names*; 2: *Kimberlite pipes*; 3: *Non-diamond-bearing kimberlite samples*; 4: *Interpreted faults*; 5*a and* 6*b*: *Meta-volcano-sediments*; 5*b*: *Dykes derived from a mixture of doleritic and diamondiferous magma*; 6*a and* 7*b*: *Argillite-type metasediments*; 7*a and* 8*b*: *Granitic intrusions and Neoproterozoic sedimentary cover*; 8*a and* 9*b*: *Dolerites*.

Aeromagnetic structures reveal several faults directions. The central part of the zone is marked by NE-SW to N-S structures, ending in a ponytail towards Koféba. E-W and NW-SE structures are also present throughout the zone. All these structures can be observed in the Birimian domain. Only NW-SE directions predominate in the Neoproterozoic sedimentary cover.

The processing carried out (DZ map obtained) has enabled us to draw up a synthesis structural model which suggests that the known kimberlite pipes are located close to the structures, or at the junction with other structural elements, and therefore at depth. These structures, and some kimberlite pipes, are also associated with doleritic dykes. Most of the known pipes seem to trend in a NW-SE direction, following the magnetic structures and supposedly derived from a mixture of doleritic and kimberlitic magma.

Indeed, many relationships between dolerites (or diabases) have been described in Canada (as xenoliths in kimberlites) [45], Russia [46], and West Africa [47]. So, taking into account the relationships between pipes and dolerites, we have a good correlation between the two.

Taking into account geochemical data, particularly from the dolerites of the Kenieba kimberlite field, and integrating them with geophysical and structural data would increase the potential for the discovery of new diamond exploration targets in the study area.

6. Conclusions

This study is based on the use of airborne geophysical data as a tool in diamond exploration in southwest Mali.

The methodology adopted in this work consisted in reprocessing the available aeromagnetic data, followed by a geological field survey.

Based on analysis of the airborne magnetic map, we have demonstrated for the first time in Mali a control model for structures associated with kimberlite pipes and their relationship with dolerite dykes. The results of this model have made it possible to locate kimberlites near or at the junction of structures oriented along NE-SW and NW-SE directions. Indeed, the majority of known pipes appear to be aligned in a NW-SE direction along the magnetic structures, possibly resulting from the injection of kimberlite and dolerite magmas.

However, the quality of these data can be improved by integrating geochemical data on the dolerites located near the kimberlite field.

Acknowledgements

This study was initiated as part of the thesis of Mr. Traore Baco at the Polytechnic Doctoral School of INP-HB in Yamoussoukro, Côte d'Ivoire. Thanks to funding from the EurekaGeo Consulting Company of Bamako, in particular the field works. We would like to say a big thank you to the Manager of this company, Dr. Sangare Souleymane.

Conflicts of Interest

The authors declare no conflicts of interest regarding the publication of this paper.

References

[1] Sangaré, S. and Diallo, T. (1998) Mali Diamond Exploration B.V. MaDE. Rapport annuel 1997-Bafoulabé-Kenieba Concession. Arrêté No 96-0068/MMEH-SG.

[2] Bardet, M.G. and Vachette, M. (1966) Détermination d'âges de kimberlites de l'ouest africain et essai d'interprétation des datations des diverses venues diamantifères dans le monde. BRGM Rapport inédit DS 66 A 59, 15 p.

[3] Jessell, M., Santoul, J., Baratoux, L., Youbi, N., Ernst, R.E., Metelka, V., Miller, J. and Perrouty, S. (2015) An Updated Map of West African Mafic Dykes. *Journal of African Earth Sciences*, **112**, 440-450. https://doi.org/10.1016/j.jafrearsci.2015.01.007

[4] Jessell, M.W., Begg, G.C. and Miller, M.S. (2016) The Geophysical Signatures of the West African Craton. *Precambrian Research*, **274**, 3-24. https://doi.org/10.1016/j.precamres.2015.08.010

[5] Baratoux, L., Söderlund, U., Ernst, R.E., de Roever, E., Jessell, M., Kamo, W.S., Naba, S., Perrouty, S., Metelka, V., Yatte, D., Grenholm, M., Diallo, D.P., Ndiaye, P.M., Dioh, E., Cournède, C., Benoit, M., Baratoux, D., Youbi, N., Rousse, S. and Bendaoud, A. (2019) New U-Pb Baddeleyite Ages of Mafic Dyke Swarms of the West African and Amazonian Cratons: Implication for Their Configuration in Supercontinents through Time. In: Srivastava, R.K., Ernst, R.E. and Peng, P., Eds., *Dyke Swarms of the World*: *A Modern Perspective*, Springer, Singapore, 263-314. https://doi.org/10.1007/978-981-13-1666-1_7

[6] Villeneuve, M. (2008) Review of the Orogenic Belts on the Western Side of the West African Craton: The Bassarides, Rokelides and Mauritanides. Geological Society, London, Special Publications, No. 297, 169-201. https://doi.org/10.1144/SP297.8

[7] Diallo, M., Baratoux, L., Dufréchou, G., Jessell, M.W., Vanderhaeghe, O., Lyb, S. and Baratoux, D. (2020) Structure of the Paleoproterozoic Kédougou-Kenieba Inlier (Senegal-Mali) Deduced from Gravity and Aeromagnetic Data. *Journal of African Earth Sciences*, **162**, Article ID: 103732. https://doi.org/10.1016/j.jafrearsci.2019.103732

[8] Wane, O., Liégeois, J.-P., Thébaud, N., Miller, J., Metelka, V. and Jessel, M. (2018) The Onset of Eburnean Collision with the Kenema-Man Craton Evidenced by Plutonic and Volcanosedimentary Rock Record of the Massigui Region, Southern Mali. *Precambrian Research*, **305**, 444-478. https://doi.org/10.1016/j.precamres.2017.11.008

[9] Grenholm, M., Jessel, M. and Thébaud, N. (2019) A Geodynamic Model for the Paleoproterozoic (ca. 2.27-1.96 Ga) Birimian Orogen of the Southern West African Craton—Insights into an Evolving Accretionary-Collisional Orogenic System. *Earth-Science Reviews*, **192**, 138-193. https://doi.org/10.1016/j.earscirev.2019.02.006

[10] Bassot, J.P. (1966) Etude géologique du Sénégal oriental et de ses confins Guinéo Maliens. Mém. B.R.G.M., 40, 332 p.

[11] Klöckner Industrie (1989) Etude géologique des fenêtres protérozoïques inférieures du secteur du projet (Kayes, Kenieba). Rapp. Techn., DNGM, Bamako, Mali, n˚1372.

[12] Chirico, P.G., Barthélémy, F. and Koné, F. (2013) Les ressources potentielles en diamants alluviaux et l'évaluation de la capacité de production du Mali. U.S. Geo-

logical Survey Scientific Investigations. Report 2010-5044, 23 p. http://pubs.usgs.gov/sir/2010/5044/ https://doi.org/10.3133/sir20105044

[13] Feybesse, J.L. (2006) Geological Synthesis of the Malian Birimian. Edition Sysmin. Unpublished Report.

[14] Chorlton, L.B. (2007) Generalized Geology of the World: Bedrock Domains and Major Faults in GIS Format: A Small-Scale World Geology Map with an Extended Geological Attribute Database. Geol. Survey Canada, Open File 5529, 48 p.

[15] Ennih, N. and Liegeois, J.P. (2008) The Boundaries of the West African Craton, with a Special Reference to the Basement of the Moroccan Metacratonic Anti-Atlas Belt. In: Ennih, N. and Liegeois, J.-P., Eds., *The Boundaries of the West African Craton*, Geological Society, London, Special Publications, No. 297, 1-17. https://doi.org/10.1144/SP297.1

[16] Haggerty, S.E. (1982) Kimberlites in Western Liberia: An Overview of the Geological Setting in a Plate Tectonic Framework. *Journal of Geophysical Research*, **87**, 10811-10826. https://doi.org/10.1029/JB087iB13p10811

[17] Hastings, D.A. and Sharp, W.G. (1979) Matters Arising: An Alternative Hypothesis for the Origin of West African Kimberlites. *Nature*, **227**, 152-153. https://doi.org/10.1038/277152c0

[18] Allialy, M.E. (2006) Pétrologie et géochimie des kimberlites diamantifères de Séguéla (Centre-Ouest de la Côte d'Ivoire). Thèse de doctorat, Université de Cocody (Côte d'Ivoire), Cocody, 184 p.

[19] Pouclet, A., Allialy, M.E., Daouda-Yao, B. and Esso, B. (2004) Découverte d'un diatrème de kimberlite diamantifère à Séguéla en Côte-d'Ivoire. *C. R. Geoscience*, **336**, 9-17. https://doi.org/10.1016/j.crte.2003.10.012

[20] Allialy, M.E., Djro, S.C., Houssou, N., Kouamelan, A.N., Batumike, J., Coulibaly, Y., Gnanzou, A., Boya, T. and Gbelé, O. (2017) Petrology and Geochemistry of Ultramafic Xenoliths Cumulats Related to Seguela Diamandifeous Kimberlite and Lamproite (Central-Western of Côte d'Ivoire). *International Research Journal of Natural and Applied Sciences*, **4**, 363-383.

[21] Yoboue, K.K.M. (2017) La question de la remédiation environnementale résultant de l'exploitation artisanale, à petite échelle du diamant: Cas de l'Union du Fleuve Mano. Thèse de doctorat, Université de Toulouse (France), Toulouse, 277 p.

[22] Bardet, M.G. (1974) Géologie du Diamant, Deuxième Partie: Gisements de Diamant d'Afrique. Ed. BRGM, 83, 223 p.

[23] Gerard, A. and Griveau, P. (1972) Quantitative Interpretation of Gravity or Magnetic Fields from Transformed Maps of the Field's First Vertical Derivative. *Geophysical*, **20**, 459-481. https://doi.org/10.1111/j.1365-2478.1972.tb00648.x

[24] Gerard, A. and Debeglia, N. (1975) Automatic Three-Dimensional Modeling for the Interpretation of Gravity or Magnetic Anomalies. *Geophysics*, **40**, 1014-1034. https://doi.org/10.1190/1.1440578

[25] Bhattacharyya, B. (1978) Computer Modeling in Gravity and Magnetic Interpretation. *Geophysics*, **43**, 912-929. https://doi.org/10.1190/1.1440873

[26] Pal, P.C., Khurana, K. and Unnikrishnan, P. (1979) Two Examples of Spectral Approach to Source Depth Estimation in Gravity and Magnetic. *Pageoph*, **117**, 772-783. https://doi.org/10.1007/BF00879978

[27] Reeves, C. (2005) Aeromagnetic Surveys: Principles, Practice and Interpretation. Earthworks éd., Geosoft, Witwatersrand, 155.

[28] Njandjock, P., Manguelle-Dicoum, E., Ndougsa-Mbarga, T. and Tabod, C.T. (2006) Spectral Analysis and Gravity Modelling in the Yagoua, Cameroon, Sedimentary Basin. *Geofísica Internacional*, **45**, 209-215. https://doi.org/10.22201/igeof.00167169p.2006.45.3.206

[29] Bikoro-Bi-Alou, M., Ndougsa-Mbarga, T. and Tabod, T.C. (2014) Quantitative Interpretation of Magnetic Anomalies in Ebolowa-Djoum Area (Southern Cameroon). G*eophysica*, **51**, 11-25.

[30] Abate Essi, J.M., Marcel, J., Diab, A., Atangana, J.Q.Y., Angue, M.A. and Ondoa, J.M. (2019) Gravity Modeling of the Au-U Mineralized Crust at the North-Central Cameroon Illustrating Crustal Permeability. *Natural Resources Research*, **50**, 473-497. https://doi.org/10.1007/s11053-019-09506-4

[31] Njeudjang, K., Kana, J.D., Tom, A., Abate Essi, J.M., Djongyang, N. and Tchinda, R. (2020) Curie Point Depth and Heat Flow Deduced from Spectral Analysis of Magnetic Data over Adamawa Volcanic Region (Northern Cameroon): Geothermal Implications. *SN Applied Sciences*, **2**, Article No. 1330. https://doi.org/10.1007/s42452-020-3099-z

[32] Ndam Njikam, M.M., Meying, A., Zanga Amougou, A. and Ngon Ngon, G.F. (2023) Mapping Transpressional and Transtensional Relay Zones by Coupling Geological and Geophysical Field Data: The Case of the Central Cameroon Shear Zone in the Mbere Administrative Division of the Adamawa Region in Cameroon. *Journal of African Earth Sciences*, **199**, Article ID: 104816. https://doi.org/10.1016/j.jafrearsci.2022.104816

[33] Saada, A.S. (2016) Edge Detection and Depth Estimation of Galala El Bahariya Plateau, Eastern Desert-Egypt, from Aeromagnetic Data. *Geomechanics and Geophysics for Geo-Energy and Geo-Resources*, **2**, 25-41. https://doi.org/10.1007/s40948-015-0019-6

[34] Blakely, R.J. (1995) Potential Theory in Gravity and Magnetic Applications. Cambridge University Press, New York, 435 p. https://doi.org/10.1017/CBO9780511549816

[35] Mounir, A., Ahmed, M. and Mustapha, M. (2012) Contribution of the Airborne Aeromagnetic Mapping to the Structural Identification of the Aquifer System of the Oasis Springs of Figuig, Morocco. *Bulletin de l'Institut Scientifique*, *Rabat*, *Section Sciences de la Terre*, **34**, 29-40.

[36] Nabighian, M. (1972) The Analytic Signal of Two-Dimensional Magnetic Bodies with Polygonal Cross-Section: Its Properties and Use for Automated Anomaly Interpretation. *Geophysics*, **37**, 507-517. https://doi.org/10.1190/1.1440276

[37] Nabighian, M. (1974) Additional Comments on the Analytic Signal of Two-Dimensional Magnetic Bodies with Polygonal Cross-Section. *Geophysics*, **39**, 85-92. https://doi.org/10.1190/1.1440416

[38] Nabighian, M. (1984) Toward a Three-Dimensional Automatic Interpretation of Potential Field Data via Generalized Hilbert Transforms: Fundamental Relations. *Geophysics*, **49**, 780-786. https://doi.org/10.1190/1.1441706

[39] Meying, A., Gouet, H.D., Ndougsa Mbarga, T., Ndam Njikam, M.M. and Owono Amougou, O.U. (2019) 2.5D Modelling of Aeromagnetic Data and their Mining Implications over the Ngaoundere Area (Adamawa Province, Cameroon). *International Journal of Geosciences*, **10**, 173-192. https://doi.org/10.4236/ijg.2019.102011

[40] Essam, A., El-Masry, N., Qaddah, A., Alqahtani, F. and Mohammed, R.H.M. (2015) Magnetic and Gravity Data Analysis of Rahat Volcanic Field, El-Madinah City, Saudi Arabia. *Journal of Astronomy and Geophysics*, **4**, 154-162. https://doi.org/10.1016/j.nrjag.2015.06.006

[41] Mhiyaoui, H., Manar, A., Remmal, T., Boujamoui, M., Kamel, F.E.L., Amar, M., Mansour, M. and Hassani, I.E.A. (2016) Deep Quaternary Volcanic Structures in the Central Middle Atlas (Morocco): Contributions of Aeromagnetic Mapping. *Bulletin de l'Institut Scientifique, Rabat, Section Sciences de la Terre*, **38**, 111-125.

[42] Yandjimain, J., Ndougsa-Mbarga, T., Meying, A., Bi-Alou, M.B., Ngoumou, P.C., Assembe, S.P., Ngoh, J.D. and Owono-Amougou, O.U.I. (2017) Combination of Tilt-Angle and Euler Deconvolution Approaches to Determine Structural Features from Aeromagnetic Data Modeling over Akonolinga-Loum Area (Centre-East, Cameroon). *International Journal of Geosciences*, **8**, 925-947. https://doi.org/10.4236/ijg.2017.87053

[43] Thompson, D. (1982) A New Technique for Making Computer-Assisted Depth Estimates from Magnetic Data. *Geophysics*, **47**, 31-37. https://doi.org/10.1190/1.1441278

[44] Reid, A.B., Allsop, J.M., Granser, H., Millett, A.J. and Somerton, I.W. (1990) Magnetic Interpretation in Three Dimensions Using Euler Deconvolution. *Geophysics*, **55**, 80-91. https://doi.org/10.1190/1.1442774

[45] Schulze, D.J. (1996) Kimberlites de la région de Kirkland Lake et du lac Témiscamingue, Ontario et Québec. In: LeCheminant, A.N., Richardson, D.G., DiLabio, R.N.W. and Richardson, K.A., Eds., *La recherche de diamants au Canada*, Commission Géologique du Canada, Ottawa, Dossier Public 3228, 73-78. https://doi.org/10.4095/210969

[46] Tomshin, M. and Gogoleva, S. (2020) Behavior of TiO_2 in Dolerits as a Possible Search Sign for Kimberlites. *IOP Conference Series: Earth and Environmental Science*, **609**, Article ID: 012073. https://doi.org/10.1088/1755-1315/609/1/012073

[47] Rollinson, H. (2016) Archaean Crustal Evolution in West Africa: A New Synthesis of the Archaean Geology in Sierra Leone, Liberia, Guinea and Ivory Coast. *Precambrian Research*, **281**, 1-12. https://doi.org/10.1016/j.precamres.2016.05.005